

Entanglement-free Heisenberg-limited phase estimation

B. L. Higgins,¹ D. W. Berry,^{2,3} S. D. Bartlett,⁴ H. M. Wiseman,^{1,3} and G. J. Pryde¹

¹Centre for Quantum Dynamics, Griffith University, Brisbane, 4111, Australia

²Physics Department, Macquarie University, Sydney, 2109, Australia

³Centre for Quantum Computer Technology, Australia

⁴School of Physics, University of Sydney, Sydney, 2006, Australia

Measurement underpins all quantitative science, and advances in precision measurement have consistently led to new scientific discoveries. A key example is the measurement of optical phase, used in length metrology and myriad other applications. At the fundamental level, measurement precision is limited by the number N of quantum resources (e.g. photons) that are used. Standard measurement schemes, using each resource independently, lead to a phase uncertainty scaling as $1/\sqrt{N}$ — the standard quantum limit (SQL). However, it has long been conjectured^{1,2} that one should be able to achieve a precision limited only by the Heisenberg uncertainty principle, dramatically improving the scaling to $1/N$ (ref.³). It is commonly held that to achieve this improvement requires exotic states such as the “NOON” state^{4,5}. Unfortunately, the generation of such states is extremely difficult — measurement schemes with counted photons or ions have been performed with $N \leq 6$ (refs.^{6,7,8,9,10,11,12,13,14,15}), but few have surpassed the SQL^{12,14} and none have shown Heisenberg-limited scaling. Here we perform the first experimental demonstration of a Heisenberg-limited phase estimation procedure. We replace entangled input states with multiple applications of the phase shift on *unentangled* single-photon states. We generalize Kitaev’s phase estimation algorithm¹⁶, using adaptive measurement theory^{17,18,19,20}, in order to achieve a standard deviation scaling at the Heisenberg limit. For the largest number of resources we use, $N = 378$, we estimate an unknown phase with a variance more than 10 dB below the SQL; achieving this variance would require more than 4,000 resources using standard interferometry. Our results represent a drastic reduction in the complexity of achieving quantum-enhanced measurement precision.

Recent work in quantum interferometry has focussed on n -photon NOON states^{5,6,7,8,9,10,11,12,21}, $\frac{1}{\sqrt{2}}(|n\rangle|0\rangle + |0\rangle|n\rangle)$, where the first and second kets represent the number states of the two arms of the interferometer. With this state, an improved phase sensitivity results from a decrease in the phase period from 2π to $2\pi/n$. We achieve improved phase sensitivity more simply using an insight from quantum computing. We apply Kitaev’s phase estimation algorithm^{16,22} to quantum interferometry, wherein the entangled in-

put state is replaced by multiple passes through the phase shift. The idea of using multi-pass protocols to gain a quantum advantage was proposed for the problem of aligning spatial reference frames²³, and further developed in relation to clock synchronization²⁴ and phase estimation^{25,26}. The conceptual circuit for Kitaev’s phase estimation algorithm is shown in Fig. 1a. Here we use the simplification²⁷ where measurement and control is used to implement the inverse quantum Fourier transform (QFT). The algorithm estimates a classical parameter ϕ , where $e^{i\phi}$ is an eigenvalue of a unitary operation U , to $K + 1$ bits of precision. This requires applying $K + 1$ unitaries, $U^{2^K}, U^{2^{K-1}}, \dots, U$, each controlled by a different qubit. Performing the inverse QFT and measurement on the control qubits then yields an estimate of ϕ . Optically, the control qubits may be dual-rail photonic qubits²² with the operator U inducing a phase shift in one arm. In this case, the label ϕ , on the target of U in Fig. 1, is the value of the unknown optical phase shift. By encoding a random initial phase on the qubits, the algorithm’s performance is independent of the value of ϕ . Alternatively, this encoding, and many of the gates in Fig. 1a, may be replaced by a second classical “feedback” phase θ which is adjusted according to the measurement outcomes as shown in 1b.

If a fixed probability of error in the estimate ϕ_{est} is allowed (i.e. if the uncertainty is quantified by a confidence interval), then the uncertainty of Kitaev’s phase estimation scales as 2^{-K} (ref.²²). Because the number of control photons is $N_{\text{phot}} = K + 1$, this scaling implies an exponential decrease in the phase uncertainty with increasing resources, apparently violating the Heisenberg uncertainty principle! The correct analysis, however, is as follows. Although the cost of implementing U^p can be assumed to be essentially independent of p in the context of quantum computation, in interferometry it requires p applications of the phase shift, and should thus be counted as requiring p resources²⁵. Using this definition, the total number of resources used is $N = 2^{K+1} - 1$. Then for $N \gg 1$, the uncertainty scales as $1/N$, as in the Heisenberg limit. We note that this quantification of resources in terms of the number of applications of the phase shift is the relevant one for phase estimation of sensitive (e.g., biological) samples, wherein the goal is to pass as little light through the sample as is necessary.

However, if $\Delta\phi_{\text{est}}$ is taken to be the standard deviation — the usual measure of uncertainty — then Kitaev’s algorithm does not scale as $1/N$. Rather, we have shown analytically that it asymptotes as $\sqrt{2}/\sqrt{N}$, the same scal-

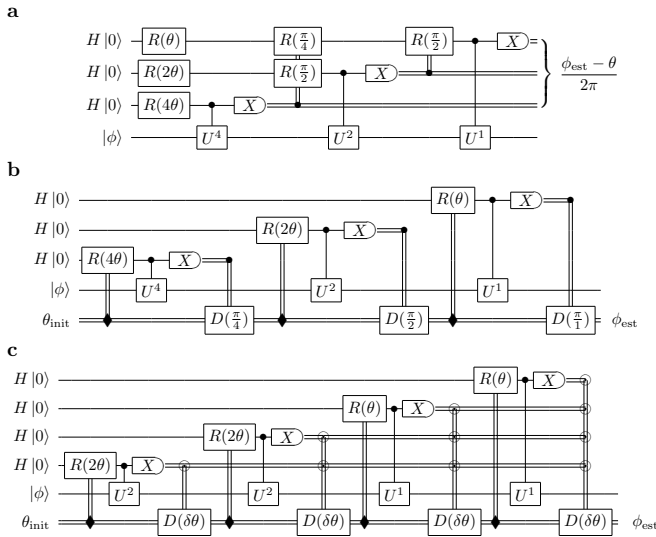


FIG. 1: Quantum circuit diagrams of Kitaev’s phase estimation algorithm and our generalization. **a**, Kitaev’s estimation algorithm¹⁶ with the inverse quantum Fourier transform implemented with measurement and classical feedback²⁷. Qubits, initially in the $H|0\rangle = \frac{1}{\sqrt{2}}(|0\rangle + |1\rangle)$ state, control unitary operations U^p on the target $|\phi\rangle$. This induces a phase shift $e^{ip\phi}$ on the $|1\rangle$ component of the control. A random initial phase θ is first encoded in these qubits to ensure sensitivity independent of ϕ . Additional phase shifts (where $R(\theta) = \exp(i\theta|0\rangle\langle 0|)$) are applied, conditional on successive measurement results. These measurements in the $X = \hat{\sigma}_x$ basis together yield the binary digits of $(\phi_{\text{est}} - \theta)/2\pi$, where ϕ_{est} is an estimate of the phase shift. In general, $K + 1$ control qubits are used to control orders of phase shift up to U^{2^K} to obtain $K + 1$ binary digits of precision (here $K = 2$). **b**, We implement the random initial phase, now θ_{init} , and the feedback operations on the control qubits, by coupling them to a common element, the “feedback phase” θ , represented by the lowest rail. This is a classical real parameter whose value is changed by π/p (as indicated by $D(\frac{\pi}{p})$), controlled by the results of measurements. It determines (as indicated by the \blacklozenge control symbol) phase-shifts $R(p\theta)$ on the qubits. Logically, this circuit is equivalent to that in **a**. **c**, Generalization of the circuit to include multiple control qubits M for each order of the phase U^p , shown for $K = 1$ and $M = 2$. The feedback phase is adjusted by an amount $\delta\theta$, controlled by all previous measurement results via a Bayesian algorithm. This general multi-bit conditioning is represented by the symbol \odot . For the final adjustment, $\delta\theta = \phi_{\text{est}} - \theta$, so the value of θ that is read out is equal to the best estimate of the phase given all the data. This adaptive algorithm no longer exactly implements the inverse QFT, but nevertheless achieves Heisenberg scaling for $M \geq 4$.

ing as the SQL! (See also ref.²¹.) The broad wings of the distribution of phase estimates are not due to any deficiency in the estimation procedure — the QFT is optimal — but rather are a consequence of the sequence of phase shifts on the photons, $2^K\phi, 2^{K-1}\phi, \dots, \phi$. A key idea to address this problem is to employ M copies of the control photon at each phase shift^{23,24,25}. For $M > 1$ one

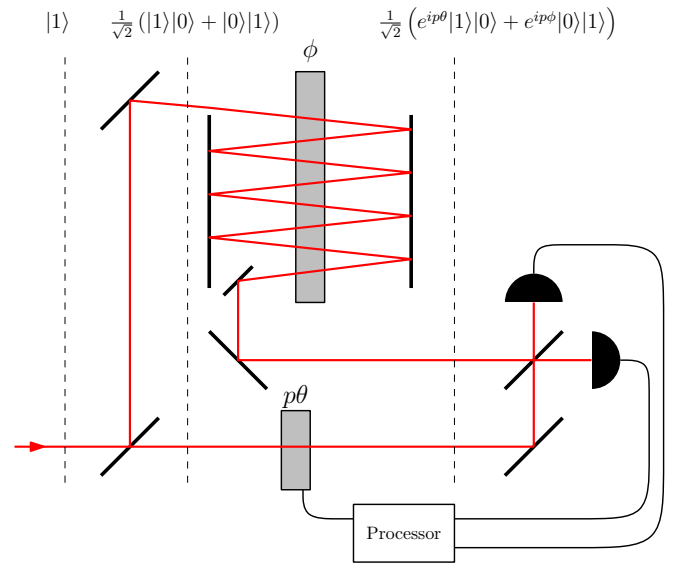


FIG. 2: Conceptual diagram of the algorithm’s implementation as a Mach-Zehnder interferometer, equivalent to the scheme in Fig. 1c. The photon-number quantum states at key points in the algorithm are provided. The first beam splitter implements the Hadamard operator on incident photons. The large phase-shift element implements the ϕ phase shift on logical $|1\rangle$ states, configured such that a photon passes an adjustable p times ($p = 8$ shown). The small phase-shift element implements the adjustable $p\theta$ phase shift on logical $|0\rangle$ states. The final beam splitter and single photon detectors implement a $\hat{\sigma}_x$ measurement, the result of which is fed into the processor which determines how to adjust θ prior to the next photon input.

cannot perform an exact QFT using only single-photon operations. However, one can perform it approximately using the adaptive phase estimation scheme of ref.¹⁸, as shown in Fig. 1c for $M = 2$. This approximation, as well as the fact that the sequence of phase shifts is not exactly equivalent to the optimal state of ref.¹⁸, causes a constant factor overhead in the uncertainty relative to the Heisenberg limit $\Delta\phi_{\text{HL}} = \tan(\pi/(N + 2)) \sim \pi/N$ (refs.^{18,28}). For instance, we find by numerical simulation that for $M = 6$, $\Delta\phi_{\text{est}} \sim 1.56\pi/N$ for $N \gg 1$.

A conceptual implementation of this generalization of Kitaev’s algorithm is shown in Fig. 2. The algorithm works as follows: A photon is converted to the state $\frac{1}{\sqrt{2}}(|1\rangle|0\rangle + |0\rangle|1\rangle)$ by the first beam splitter. After passing through the phase shift $p = 2^K$ times the state evolves to $\frac{1}{\sqrt{2}}(e^{ip\theta}|1\rangle|0\rangle + e^{ip\phi}|0\rangle|1\rangle)$. The photon is then detected after the modes are recombined on the second beam splitter. The result is used to provide a Bayesian update to a probability distribution $P(\phi)$ which represents knowledge about ϕ . We take this distribution to be initially flat.

This process is repeated M times, so that M independent photons go through 2^K passes in sequence. Quantifying a *resource* as a *single* pass of a photon through the phase shift, each photon in this stage corresponds to 2^K

resources. Following these M photons, another M photons undergo the same process at $p = 2^{K-1}$ passes, and so on for $p = 2^{K-2}, \dots, 2^0$. Thus a total of $M(K+1)$ photons and $N = M(2^{K+1} - 1)$ resources are used. The probability distribution P is updated for each photon measurement. The value of the feedback phase θ is random for the first photon only. Thereafter it is chosen, based upon P (that is, upon all preceding results), to minimize the expected phase variance after the next detection¹⁸.

This algorithm reduces to Kitaev's algorithm for $M = 1$. We have shown analytically that this algorithm gives a standard deviation of estimates scaling as the SQL for $M = 2$ as well as $M = 1$, and numerical simulations demonstrate a Heisenberg-limited scaling for $M \geq 4$ (for N up to 4×10^6 and M up to 8).

Note that a single photon with p passes through the unknown phase shift is exactly equivalent to a NOON state with $n = p$ photons, and involves exactly the same number of resources. A single NOON state such as this yields at most one bit of information⁴, and only about ϕ modulo $2\pi/n$. It has been shown numerically²¹ that a sequence of NOON states, with n as well as θ chosen adaptively, achieves Heisenberg-limited scaling, but only for $N > 100$. Our generalized algorithm, which is simpler, can also be applied to NOON states, and directly achieves Heisenberg-limited scaling. Even if high- n NOON states could be produced, however, they require high- n photon-number-resolving detectors, and are proportionately more sensitive to detector inefficiency than single photons with multiple passes through the phase shift.

We demonstrate our single-photon algorithm using a common-spatial-mode polarization interferometer, as shown in Fig. 3. The two arms of the interferometer are the right ($|R\rangle$) and left ($|L\rangle$) polarization modes. The unknown phase ϕ is implemented as a birefringent half-wave plate (HWP) 50 mm in diameter. A single photon passing through this HWP undergoes a rotation of its polarization such that $\frac{1}{\sqrt{2}}(|R\rangle + |L\rangle) \rightarrow \frac{1}{\sqrt{2}}(|R\rangle + e^{i\phi}|L\rangle)$ for a HWP setting of $\phi/4$. Two 50 mm mirrors are placed on either side allowing a single photon to pass through the ϕ HWP multiple times. The feedback phase is implemented as another HWP mounted in a motorized rotation stage before the unknown phase and mirrors. We use a fixed phase ϕ , but the use of a uniformly-distributed random initial feedback phase is equivalent to performing the protocol over the full range of system phases, $\phi \in [0, 2\pi)$. Mirrors on computer-controlled, motorized translation stages are used to select the 2^k th pass for each value of k . After the interferometer, measurement is performed in the horizontal/vertical basis, corresponding to a $\hat{\sigma}_x$ measurement with respect to the $\{|R\rangle, |L\rangle\}$ basis states.

We test two versions of the algorithm: $M = 1$ (Kitaev's algorithm), and $M = 6$ (chosen for its robustness). For each, we vary the number of resources $N = M(2^{K+1} - 1)$ by choosing different values for the maxi-

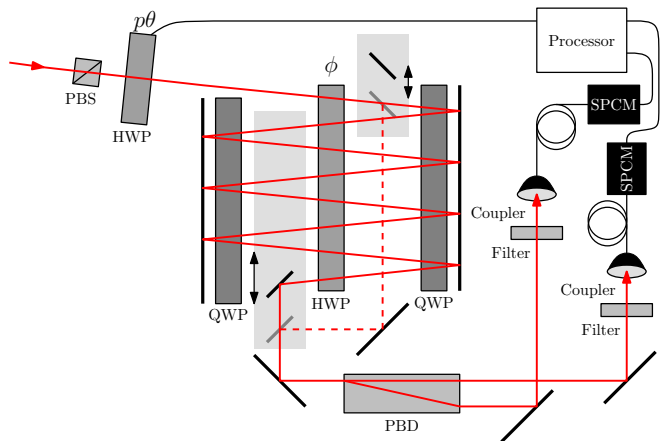


FIG. 3: Schematic of the experiment. The right-circular $|R\rangle$ and left-circular $|L\rangle$ polarization modes of a photon replace the arms of the Mach-Zehnder interferometer presented in Fig. 2. For our experiment we define $|R\rangle$ and $|L\rangle$ to be the eigenstates of $\hat{\sigma}_z$. The unknown and feedback phases are implemented as half-wave plates (HWPs). Quarter-wave plates (QWPs) set at their optic axes correct π -phase shifts on reflections. A photon enters the circuit and is horizontally polarized ($|H\rangle = \frac{1}{\sqrt{2}}(|R\rangle + |L\rangle)$) by the polarizing beam splitter (PBS). Through the circuit, the photon experiences phase shifts between left- and right-circular polarizations by the feedback wave plate ($p\theta$) and the wave plate implementing the unknown phase (ϕ). The photon passes multiple times through the unknown phase before it is selected by a mirror mounted on a motorized translation stage. The region of travel of the translatable mirrors is shown in light grey. In this figure, the photon is picked off after 8 passes. The dashed line represents the mode of the single-pass case, with the positions of the translating mirrors shown in grey. After the photon is picked off it is discriminated in the horizontal/vertical polarization basis (a $\hat{\sigma}_x$ measurement) by a polarizing beam displacer (PBD), and passes through a 10 nm bandwidth interferometric filter. It is then coupled into multimode fibre, and is detected by a single-photon counting module (SPCM). A detection in coincidence with a second photon from the spontaneous parametric downconversion source (not shown) heralds a successful measurement.

imum number of passes, 2^K , with $K \in \{0, 1, 2, 3, 4, 5\}$. We also measured the standard deviation for a non-adaptive or “standard” estimation algorithm, employing N single passes of the phase shift, with N chosen equal to the number of resources used for each of the $M = 6$ data points. In this case θ was incremented non-adaptively²⁹ by π/N from one photon to the next, to ensure a sensitivity independent of ϕ .

The experimental results are shown in Fig. 4, together with theoretical calculations. Each data point represents 1,000 phase estimates. The error bars are 95% confidence intervals determined using a studentized bootstrap on a log scale³⁰. In general, the distributions have a large positive kurtosis which emphasizes the effect of outliers — our error calculation takes this into account to provide accurate error bars.

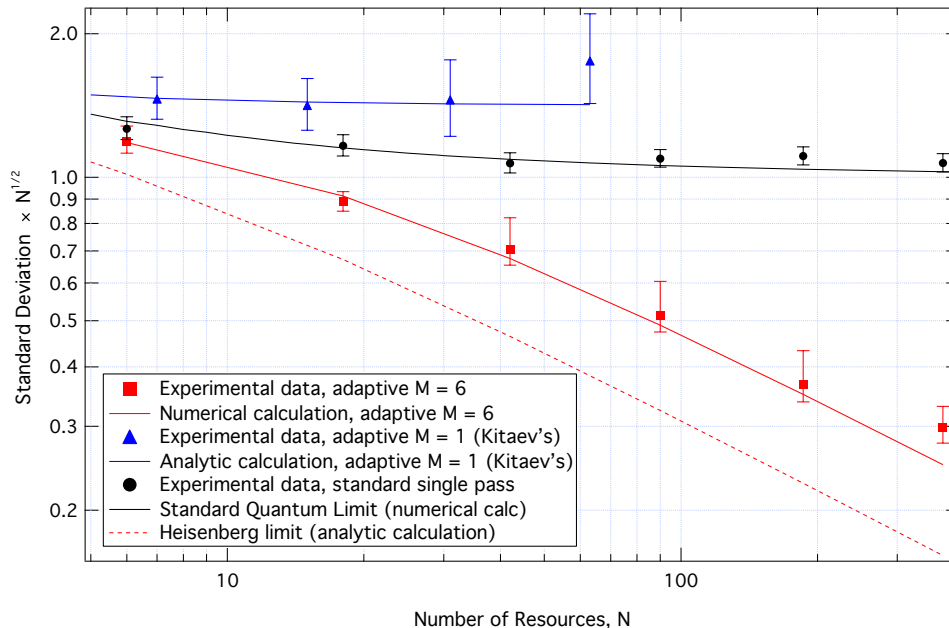


FIG. 4: Theoretical and measured standard deviations of distributions of phase estimates for varying numbers of resources N . Theoretical predictions are shown as lines, measured values as points. We compare results for standard non-adaptive phase estimation and our implementation of Kitaev’s ($M = 1$) and generalized Kitaev’s ($M = 6$) algorithms. Data points generally follow their corresponding predicted values, although the $M = 6$, $N = 378$ point and the $M = 1$, $N = 63$ point have slightly higher than expected standard deviations. We attribute this to a decrease in interferometric visibility at such large number of passes. Numerical simulations (not shown) using the experimental visibilities are consistent with this hypothesis. Theoretical predictions shown here have assumed perfect (100%) visibility for all passes. Experimentally, while visibilities for 1 to 16 passes were high (all above 98.1% and typically above 99.6%), the 32 pass case had slightly lower visibility, approximately 95.4%. This is primarily due to expansion of the beam waist and subsequent overlap of beams resulting from the long optical path length at 32 passes. Despite this, our algorithm clearly has a lower standard deviation in phase estimates than both the SQL and Kitaev’s algorithm (which has SQL scaling). For large N , the standard deviation curve for the adaptive algorithm is parallel to the Heisenberg limit, with a small overhead factor of about 1.56.

The results of the non-adaptive phase estimation algorithm follow the SQL, as expected. Notably, the standard deviations of the $M = 1$ (Kitaev’s) case also follow an SQL scaling. Most importantly, there is a clear Heisenberg scaling, $\Delta\phi_{\text{est}} \propto 1/N$, of our adaptive multi-pass algorithm for $M = 6$. Our data are consistent with the predicted overhead factor of 1.56 relative to the asymptotic Heisenberg-limited standard deviation π/N . Despite this constant overhead, our phase estimates clearly surpass the SQL. For example, where we have demonstrated the use of 378 resources in our algorithm (corresponding to a maximum of 32 passes), 4,333 resources would be required using standard techniques to achieve the same uncertainty.

We have introduced a new algorithm for phase estimation, generalizing Kitaev’s algorithm, which requires no entanglement to achieve Heisenberg-limited scaling independent of ϕ . Our algorithm uses single-photon Fock states, multiple passes and adaptive measurement. We have used our algorithm to successfully demonstrate the first measurement with Heisenberg-limited scaling. This technique has promise for a wide range of metrology tasks, especially in light of continued development of

high-flux single photon sources and efficient detectors.

Methods

Source. A type-I Bismuth borate spontaneous parametric down-conversion source, pumped by a frequency-doubled modelocked Ti:Sapphire laser, supplies pairs of 820 nm, 2 nm-bandwidth single photons in the state $|HH\rangle$. One photon is guided to the experiment through a single-mode optical fibre, the other is guided straight to a single photon counting module (SPCM). After the interferometer, measurement is performed in the horizontal/vertical basis with a high-contrast-ratio calcite polarising beam displacer. The two outputs of the beam displacer are coupled into multimode optical fibres and sent to SPCMs. Each output is filtered with 10 nm-bandwidth interference filters to reject background light. A successful measurement is heralded by a coincidence between the directly-detected photon and either of the output detectors — coincidence detection reduces background and dark counts, ensuring high-fidelity conditional single photons in the experiment.

Interferometer. To correct the unwanted π -phase shift on reflection, a quarter-wave plate (QWP), set to its optic axis, is inserted before each of the 50 mm mirrors.

For logistical reasons, we use 25 mm diameter QWPs for most experiments, but 50 mm diameter wave plates for the $K = 5$ cases. The wave plates are nominally identical except for their diameter. The QWPs did introduce a technical challenge — because of the large-diameter optics, and the need to use all of the clear aperture to obtain multiple reflections, we used mountings that did not allow easy calibration and adjustment of the QWPs. This in turn led to small additional phase shifts from the QWPs that were dependent upon the number of passes.

This problem is easily modelled and is not fundamental.

Statistics for phase. For a cyclic variable ϕ with distribution P , an appropriate measure of error in the estimate ϕ_{est} is $V = \langle \cos(\phi - \phi_{\text{est}}) \rangle_P^{-2} - 1$. This is minimized for the best estimate, $\phi_{\text{est}} = \arg(\langle \exp(i\phi) \rangle_P)$, which is the one we use. In this case V is called the Holevo variance²⁸. When we apply the terms *variance* and *standard deviation* to a phase, these are to be understood as the Holevo variance and its square root respectively.

-
- ¹ Caves, C. M. Quantum-mechanical noise in an interferometer. *Phys. Rev. D* **23**, 1693–1708 (1981).
- ² Yurke, B., McCall, S. L. & Klauder, J. R. SU(2) and SU(1,1) interferometers. *Phys. Rev. A* **33**, 4033–4054 (1986).
- ³ Giovannetti, V., Lloyd, S. & Maccone, L. Quantum-Enhanced Measurements: Beating the Standard Quantum Limit. *Science* **306**, 1330–1336 (2004).
- ⁴ Bollinger, J. J., Itano, W. M., Wineland, D. J. & Heinzen, D. J. Optimal frequency measurements with maximally correlated states. *Phys. Rev. A* **54**, R4649–R4652 (1996).
- ⁵ Lee, H., Kok, P. & Dowling, J. P. A quantum Rosetta stone for interferometry. *J. Mod. Opt.* **49**, 2325–2338 (2002).
- ⁶ Rarity, J. G. *et al.* Two-Photon Interference in a Mach-Zehnder Interferometer. *Phys. Rev. Lett.* **65**, 1348–1351 (1990).
- ⁷ Fonseca, E. J. S., Monken, C. H. & Pádua, S. Measurement of the de Broglie Wavelength of a Multiphoton Wave Packet. *Phys. Rev. Lett.* **82**, 2868–2871 (1999).
- ⁸ Edamatsu, K., Shimizu, R. & Itoh, T. Measurement of the Photonic de Broglie Wavelength of Entangled Photon Pairs Generated by Spontaneous Parametric Down-Conversion. *Phys. Rev. Lett.* **89**, 213601 (2002).
- ⁹ Walther, P. *et al.* De Broglie wavelength of a non-local four-photon state. *Nature* **429**, 158–161 (2004).
- ¹⁰ Mitchell, M. W., Lundeen, J. S. & Steinberg, A. M. Super-resolving phase measurements with a multiphoton entangled state. *Nature* **429**, 161–164 (2004).
- ¹¹ Eisenberg, H. S., Hodelin, J. F., Houry, G. & Bouwmeester, D. Multiphoton Path Entanglement by Nonlocal Bunching. *Phys. Rev. Lett.* **94**, 090502 (2005).
- ¹² Leibfried, D. *et al.* Creation of a six-atom ‘Schrödinger cat’ state. *Nature* **438**, 639–642 (2005).
- ¹³ Sun, F. W., Liu, B. H., Huang, Y. F., Ou, Z. Y. & Guo, G. C. Observation of the four-photon de Broglie wavelength by state-projection measurement. *Phys. Rev. A* **74**, 033812 (2006).
- ¹⁴ Nagata, T., Okamoto, R., O’Brien, J. L., Sasaki, K. & Takeuchi, S. Beating the Standard Quantum Limit with Four-Entangled Photons. *Science* **316**, 726–729 (2007).
- ¹⁵ Resch, K. J. *et al.* Time-Reversal and Super-Resolving Phase Measurements. *Phys. Rev. Lett.* **98**, 223601 (2007).
- ¹⁶ Kitaev, A. Y. Quantum measurements and the Abelian Stabilizer Problem. *Electronic Colloquium on Computational Complexity* **3**, 3 (1996).
- ¹⁷ Wiseman, H. M. Adaptive phase measurements of optical modes: Going beyond the marginal Q distribution. *Phys. Rev. Lett.* **75**, 4587–4590 (1995).
- ¹⁸ Berry, D. W. & Wiseman, H. M. Optimal States and Almost Optimal Adaptive Measurements for Quantum Interferometry. *Phys. Rev. Lett.* **85**, 5098–5101 (2000).
- ¹⁹ Armen, M. A., Au, J. K., Stockton, J. K., Doherty, A. C. & Mabuchi, H. Adaptive homodyne measurement of optical phase. *Phys. Rev. Lett.* **89**, 133602 (2002).
- ²⁰ Cook, R. L., Martin, P. J. & Geremia, J. M. Optical coherent state discrimination using a closed-loop quantum measurement. *Nature* **446**, 774–777 (2007).
- ²¹ Mitchell, M. W. Metrology with entangled states. *Proc. SPIE* **5893**, 589310 (2005).
- ²² Nielsen, M. A. & Chuang, I. L. *Quantum Computation and Quantum Information* (Cambridge Univ. Press, Cambridge, 2000).
- ²³ Rudolph, T. & Grover, L. Quantum Communication Complexity of Establishing a Shared Reference Frame. *Phys. Rev. Lett.* **91**, 217905 (2003).
- ²⁴ de Burgh, M. & Bartlett, S. D. Quantum methods for clock synchronization: Beating the standard quantum limit without entanglement. *Phys. Rev. A* **72**, 042301 (2005).
- ²⁵ Giovannetti, V., Lloyd, S. & Maccone, L. Quantum Metrology. *Phys. Rev. Lett.* **96**, 010401 (2006).
- ²⁶ van Dam, W., D’Ariano, G. M., Ekert, A., Macchiavello, C. & Mosca, M. Optimal quantum circuits for general phase estimation. *Phys. Rev. Lett.* **98**, 090501 (2007).
- ²⁷ Griffiths, R. B. & Niu, C.-S. Semiclassical Fourier Transform for Quantum Computation. *Phys. Rev. Lett.* **76**, 3228–3231 (1996).
- ²⁸ Wiseman, H. M. & Killip, R. B. Adaptive single-shot phase measurements: A semiclassical approach. *Phys. Rev. A* **56**, 944–957 (1997).
- ²⁹ Hradil, Z. *et al.* Quantum Phase in Interferometry. *Phys. Rev. Lett.* **76**, 4295–4298 (1996).
- ³⁰ Davison, A. C. & Hinkley, D. V. *Bootstrap Methods and Their Application* (Cambridge Univ. Press, Cambridge, 1997).

Acknowledgements We thank M. Mitchell, D. Bulger and S. Lo for discussions. This work was supported by the Australian Research Council and the Queensland State Government.

Author information Correspondence should be addressed to G.J.P. (email: g.pryde@griffith.edu.au).